irep INTERNATIONAL INSTITUTE
FOR RESEARCH AND EDUCATION
IN POWER SYSTEM DYNAMICS

NATIONAL TECHNICAL
UNIVERSITY OF
ATHENS

BULK POWER SYSTEMS DYNAMICS AND CONTROL IV RESTRUCTURING

Symposium Proceedings

Edited by L. H. Fink and C. D. Vournas

Santorini, Greece
August 23 – 28, 1998

Table of Contents

TRANSIENT STABILITY-CONSTRAINED GENERATION RESCHEDULING

Daniel Ruiz-Vega, Arlan Bettiol *, Damien Ernst, Louis Wehenkel **, Mania Pavella

University of Liège, Department of Electrical Engineering,
Sart Tilman B28, B-4000 Liège, Belgium

* On leave from University of Vale do Itajaí (UNIVALI), Brazil
** Research Associate F.N.R.S.

Abstract. This paper deals with the derivation of on-line techniques for transient stability assessment and control, directly relating to the available transfer capability (ATC) arena. The developments rely on SIME, a hybrid direct – time-domain method, along with advances obtained quite recently. These advances concern compensation schemes, which yield techniques for ultra-fast filtering, and for generation control. In turn, these techniques allow improvements of the "maximum allowable transfer" (MAT) method recently proposed. The paper provides a unified view of the various techniques, their advances and their applications. It illustrates them and assesses their performances by means of simulations performed on a real-world power system.

Keywords. Generation rescheduling; On-line transient stability assessment and control; SIME; contingency filtering; real-time preventive control; available transfer capability; transient stability-constrained maximum allowable transfer; dynamic security assessment.

1 Introduction

One of the major challenges the deregulated electric industry faces in the ATC arena is the determination of dynamic security limits, i.e., of voltage and transient stability limits [1]. This paper addresses issues directly relating to transient stability limits. In particular, it aims at determining on-line transient stability-limited maximum generation or transfer capability between areas.

Basically, despite their specifics, the various approaches to on-line DSA and control rely on common techniques, such as : the identification of critical contingencies by screening a list of plausible ones, the accurate assessment of the critical contingencies, and the assessment of control actions necessary to stabilize them. Moreover, these techiques must comply with real-time computing requirements.

The conventional time-domain transient stability methods are unable to tackle efficiently such issues, if at all. Indeed, even the identification of the critical contingencies among a large list of dynamic ones would be too time consuming to comply with on-line requirements. As for the assessment of control actions, there is no systematic way even for a single critical contingency, not to mention for their simultaneous stabilization.

Direct-like or hybrid direct – time-domain methods are conceptually better suited for the above tasks [2 to 7]. And among such hybrid methods, those relying on a single-machine equivalent of the multimachine power system are quite appealing. Indeed, these methods allow identification of the critical machines, and interpretations provided by the equal-area criterion, which are of paramount importance [8 to 10].

The hybrid method called SIME (for SIngle-Machine Equivalent) belongs to the latter family. SIME per se may be useful to various application contexts, such as :

- planning studies, for screening thousands of contingencies and for appraising the influence of major system parameters
- operational planning, for reliability studies
- real-time operation, for deriving on-line DSA and control techniques.

This paper deals with the real-time operation context, and more specifically with techniques tailored for on-line transient stability monitoring and control.

Such techniques were developed quite recently. They concern on the one hand ultrafast contingency filtering, ranking and assessment, on the other hand generation control. The filtering techniques rely on compensation schemes proposed in Ref. [11], which also proposed a technique for controlling generation. Further, Ref. [12] has proposed the MAT method, which aims at assessing maximum allowable transfer between areas, hence its name.

This paper provides a unified view of the above advances, and suggests means of taking advantage of them to cover various needs in the field of DSA and control.

The paper is organized as follows. Section 2 outlines the SIME method per se. Section 3 presents various types of compensation schemes and suggests means of exploiting them for both contingency screening and controlling generation. Section 4 revisits the MAT method and takes advantage of compensation schemes to further improve its performances. Section 5 reports on simulations performed on the South-Southeast Brazilian power system, in order to illustrate the various approaches, validate them and assess performances. Finally, Section 6 discusses further applications and draws conclusions.

2 SIME's essentials

This section is transcribed from Ref. [11].

2.1 *Foundations*

Basically, SIME deals with the post-fault configuration of a power system subjected to a disturbance which presumably

drives it to instability. Under such conditions, SIME uses a time-domain program in order to : identify the mode of separation of its machines into two groups; replace these groups by successively a two-machine, then a **one-machine infinite bus (OMIB)** equivalent system; assess transient stability of this OMIB via the margins resulting from the application of the equal-area criterion [13 to 15].

The various steps of the method are briefly described below and illustrated in Figs 1, corresponding to a real stability case of the Brazilian system simulated in Section 5.

2.2 *Critical machines and OMIB*

On an unstable time-domain trajectory, the critical machines are those which cause the system to lose synchronism. To identify them, SIME observes the post-fault swing curves of the system machines computed via a time-domain program. At each step, it sorts the machines in decreasing order of their rotor angles, identifies the very first largest angular deviations (largest "gaps") between any two adjacent machines thus sorted, and considers as *candidate* critical clusters of concern those which are "above these largest gaps". The corresponding candidate OMIB's trajectories are computed as explained in §§ 2.3, 2.4. The procedure is carried out until a candidate OMIB reaches its unstable angle δ_u (defined in § 2.4) : it is then declared to be the critical OMIB.

Observe that a critical OMIB is defined only on an unstable case. By continuation, it is considered to be also valid on a borderline stable case.

Figs 1 illustrate the critical machines identification procedure.

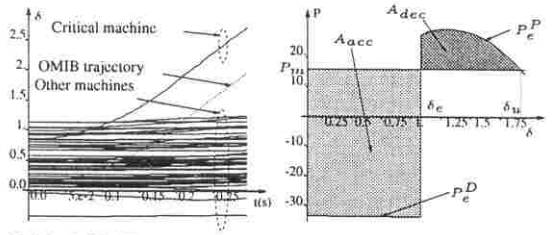

(a) Critical OMIB identification
Nr of critical m/nes : 1
Nr of non-critical m/nes : 55
---- Critical OMIB trajectory
—— Multimachine trajectories

(b) Power-angle OMIB representation
Resulting equal-area crit.
$t_e = 167$ ms ; $t_u = 360$ ms ;
(CCT = 141 ms)

Figure 1. Time-domain machines' and OMIB's trajectories; resulting equal-area criterion. Stability case Nr 672.

2.3 *Critical OMIB parameters*

Let C denote the group of critical (or advanced) machines and N that of the non-critical (or backward) machines. In Fig. 1a, the critical cluster is composed of one machine only (machine labelled 2712 in Section 5); the non-critical cluster is thus composed of 55 machines.

The corresponding critical OMIB parameters δ, ω, M, P_m, P_e are readily computed as follows.

(i) Transform the two clusters into two equivalent machines, using their corresponding partial center of angle. E.g., for cluster C this results in

$$\delta_C(t) \triangleq M_C^{-1} \sum_{k \in C} M_k \delta_k(t) \text{ with } M_C = \sum_{k \in C} M_k \ . \quad (1)$$

Similar expressions hold for cluster N, and yield the angle δ_N.

(ii) Reduce this two-machine system into an equivalent OMIB system whose rotor angle is defined by

$$\delta(t) \triangleq \delta_C(t) - \delta_N(t) \quad (2)$$

and whose rotor speed, ω, is defined in a similar way.

(iii) Define the equivalent OMIB mechanical power by

$$P_m(t) = M \left(M_C^{-1} \sum_{k \in C} P_{mk}(t) - M_N^{-1} \sum_{j \in N} P_{mj}(t) \right) \quad (3)$$

where $M = M_C M_N / (M_C + M_N)$ is the equivalent OMIB inertia coefficient. The OMIB electrical power P_e takes on a similar expression.

Fig. 1a portrays the OMIB trajectory plotted from the multimachine trajectories (swing curves).

2.4 *Calculation of stability margins*

The equation of motion of the OMIB equivalent

$$M\ddot{\delta} = M\dot{\omega} = P_m - P_e = P_a \quad (4)$$

where P_a is the accelerating power, expresses in particular its power-angle dynamics.

The well-known equal-area criterion uses the notion of stability margin :

$$\eta = A_{dec} - A_{acc} \quad (5)$$

and states that : *for a given stability scenario the OMIB system is unstable if $\eta < 0$, stable otherwise. The borderline case, $\eta = 0$, provides the limit (in)stability condition, in terms of critical clearing time or power limit.*

The above unstable and stable margins are expressed respectively by eqs (6), (7) :

$$\eta_u = -\frac{1}{2} M \omega_u^2 \quad (6)$$

$$\eta_{st} = \int_{\delta_r}^{\delta_u} |P_a| \, d\delta \ . \quad (7)$$

In these expressions,

- subscript u (for unstable) refers to the angle, δ_u, speed, ω_u, and time t_u where $P_a = 0$, $\dot{P}_a > 0$;
- subscript r (for return) refers to the angle δ_r and time t_r where δ starts decreasing and ω vanishes.

Fig. 1b illustrates the equal-area criterion in the slightly unstable case portrayed in Fig. 1a (A_{acc} is larger than A_{dec} : $\eta = -3$). Note that the computation of the unstable margin requires a time-domain simulation performed until reaching t_u . (Here, $t_u = 360$ ms).

Remark. The above considerations show that t_u is the simulation period needed to compute an unstable margin; similarly,

t_r is the simulation period needed to compute a first-swing stable margin. Observing further that the computation of a stability limit (critical clearing time or power limit) requires about 2 to 3 unstable and 1 stable margins suggests that this computation amounts to about 2 seconds of time-domain integration.[1]

2.5 *Contingency filtering, ranking, assessment*

Contingency filtering. The purpose of filtering (generally a large list of) contingencies is to discard the harmless ones (generally the major part of the list), and keep the potentially harmful contingencies for further scrutiny.

The standard "filtering SIME" procedure [14, 15] uses two margin values computed for two (relatively close) stability conditions that extrapolates or interpolates to get an approximate limit value; its comparison with a preassigned threshold value allows discarding or keeping the contingency, as appropriate.

This procedure is found to be consistently reliable. On the other hand, whenever simplified power system models make sense, substantial gains may be obtained by using a sequence of filters with increasing modeling details.

Finally, observe that screening contingencies in terms of **critical clearing times (CCTs)** is as valid but much faster than in terms of power limits. This advocates using filtering steps in terms of CCTs, then refining the assessment of the potentially harmful contingencies in terms of power limits, if necessary. This observation is on the basis of compensation schemes for controlling clearing time devised below, in § 3.1.

Contingency ranking. The severity of the potentially harmful contingencies as identified by the filtering step may further be subdivided into dangerous and non-dangerous ones.

To fix ideas, when the contingency screening is performed with detailed power system modeling, the boundary between harmless and potentially harmful contingencies may be of 200 ms; among the harmful contingencies, those whose CCT is below 10 cycles ($\approx$ 167 ms) may be declared to be dangerous.

Contingency assessment. For contingencies found by the filtering SIME to be potentially harmful, it may be worth refining their limit assessment. If the limit of interest is the CCT, this simply consists of using one margin value (i.e. one simulation) in addition to those of the filtering step; this simulation should correspond to a stable scenario, if multiswing instabilities are sought.

Another stability limit worthwhile to compute is the power limit corresponding to a given clearing time (e.g., for a clearing time of 10 cycles, i.e. 167 ms).

Yet, another interesting parameter is the stability margin, η, corresponding to a clearing time of 167 ms : dangerous contingencies will have negative margins, stable contingencies will have positive margins.

Illustration. The above contingency filtering and assessment procedures are illustrated on the stability scenario Nr 672 of the Brazilian power system. The results are portrayed in Figs 2.[2]

[1] Except whenever multiswing instability phenomena are sought, in which case an entire stable simulation is needed.

[2] Note that the margins appearing in these figures are normalized by the OMIB inertia coefficient : $\eta = -\omega_u^2/2(\text{rad/s})^2$.

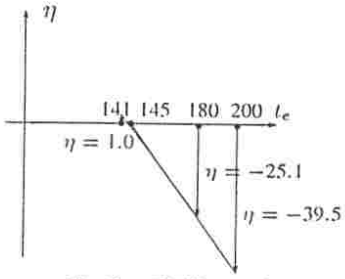

Fig. 2a CCT search under base case conditions

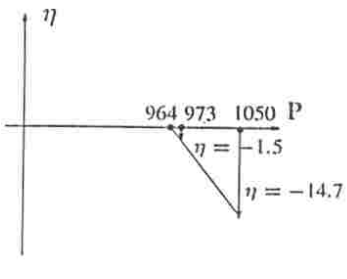

Fig. 2b Power limit search; CT = 167 ms

Figure 2. Contingency filtering and assessment

Fig. 2a shows that the filtering SIME finds a CCT of 145 ms, by extrapolating the (negative) margin values corresponding to two clearing times (CTs) : 200 ms and 180 ms. According to the threshold values chosen above, this contingency is not only a potentially harmful one, but also dangerous. Choosing an additional CT of 140 ms (smaller than 145 ms) allows refining the CCT assessment by interpolating between the positive margin and the last negative one; this yields 141 ms.

Fig. 2b illustrates a similar extrapolation procedure performed to compute the power limit corresponding to a CT of 167 ms.

Finally, under base case conditions, this stability scenario has a margin of -14.7 (rad/s)^2 for a clearing time of 167 ms (e.g., see Table 2)

3 Compensation schemes Resulting techniques

3.1 *Compensation schemes for controlling clearing time*

3.1.1 Problem statement

Given an unstable case, characterized by its clearing time (CT or t_c), and appraised by its negative margin, the purpose is to assess how much to decrease the clearing time in order to stabilize the case, i.e. to cancel out the margin.

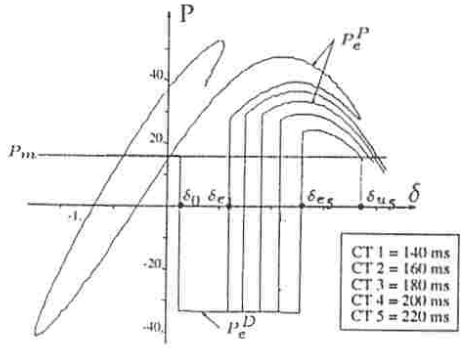

Figure 3. Curves P_m , P_e vs $\delta_e(t_e)$ for stability case Nr 672 (CCT = 141 ms). Taken from [11].

Ref. [11] has tackled this question and proposed four compensation schemes suggested by the shape of the P_e curves variation with CT (or equivalently with the clearing angle δ_e) ;

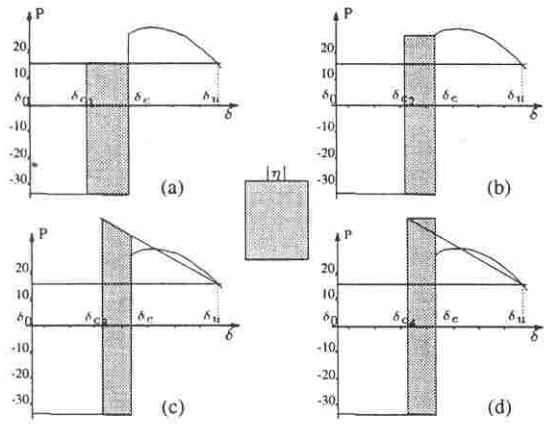

Figure 4. Four compensation schemes for CCT assessment. Stability case Nr 672.
$t_e = 167\,ms$ ($\delta_e = 0.82\,rad$); $\eta = -14.7$. Taken from [11].

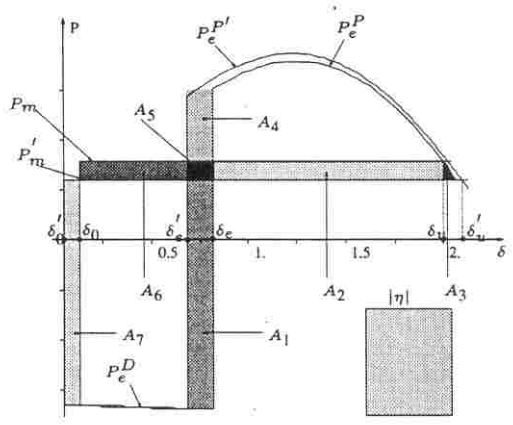

Figure 5. Compensation scheme for controlling generation. Stability case Nr 672. $t_e = 167\,ms$; $\eta = -14.7$; $P_m = 324MW$; $P_C = 1050MW$. Taken from [11]

such typical curves are drawn in Fig. 3. Figure 4 [3] portrays these compensation schemes; they are obtained by using four different ways of compensating for the margin, which is represented by the shaded rectangular area. This negative (normalized) margin amounts to -14.7 (rad/s)^2 for $t_e = 167$ ms . The margin is compensated by increasing the decelerating and/or decreasing the accelerating area. They yield four different estimated δ_{ci}'s (and hence estimated CCT_i's). Note that Figs 4a to 4d yield increasing t_{ci} values of 125, 136, 143 and 144 ms respectively; (remember, the actual CCT is 141 ms).

3.1.2 Resulting contingency filtering techniques

In § 2.5, contingency filtering was relying on CCTs obtained by interpolating or extrapolating two margin values. For example, in Fig. 2a this 2-margin filter provides an approximate CCT value of 145 ms.

In Ref. [11], a set of 20 stability scenarios were simulated, using the compensation schemes proposed above. The simulations have shown that schemes (c) and (d) provide CCTs with good accuracy; they thus seem interesting for the purpose of screening contingencies. A much broader investigation carried out in this paper and reported in Section 5, suggests that scheme (c) provides slightly smaller CCTs than scheme (d); being slightly more conservative, it is thus preferred for the purpose of filtering contingencies.

3.2 *Compensation scheme for controlling generation*

3.2.1 Problem statement

The compensation scheme proposed in this paragraph aims at stabilizing an otherwise unstable scenario, by decreasing the OMIB mechanical power. Once the amount of decrease has been determined, a rescheduling of the multimachines' generation can be performed. Thus, actually, the proposed compensation procedure addresses the following two questions : (i) how much to decrease the OMIB mechanical power ? (ii) how to convert this decrease into the actual machines' generation change ?

Figure 5 helps answer question (i). It shows that lowering the mechanical power from P_m to P'_m modifies the accelerating and decelerating areas of the OMIB $P - \delta$ representation. More precisely, it increases the decelerating area (by areas A_2 to A_5), decreases the accelerating area (A_1, A_5 and A_6), and increases the accelerating area (A_7). Thus,

$$|\eta| = \sum_{i=1}^{6} A_i - A_7 \,. \tag{8}$$

Expression (8) links directly $|\eta|$ to the amount of P_m decrease. Actually, decreasing P_m implies increasing P_e^P , thus adding one more decelerating area, say A_8 , comprised between curves $P_e^{P'}$ and P_e^P . But its computation would imply another time-domain simulation. On the other hand, neglecting A_8 gives a pessimistic assessment, i.e. an overestimation of $\Delta P_m = P_m - P'_m$, which, however, is rather minor (a small percentage, see footnote [5]).

The computation of areas (A_1 to A_6) is straightforward. Computation of area A_7 merely requires computation of δ'_0 ; it may be neglected in a first approximation, inasmuch as A_7 partly counterbalances the effect of A_8 .

3.2.2 Resulting generation rescheduling

To answer question (ii) of § 3.2.1, i.e., convert the decrease of the OMIB mechanical power, ΔP_m , observe that the distribution of the OMIB ΔP_m among actual machines' generation must obey eq. (3). This equation suggests that decreasing P_m implies decreasing generation of **critical machines (CMs)** and increasing generation of **non critical machines (NMs)** according to :

$$-\Delta P_m = -\frac{M_N}{M_N + M_C}\Delta P_C + \frac{M_C}{M_N + M_C}\Delta P_N \tag{9}$$

where
$$\Delta P_C = \sum_{k \in C} \Delta P_{mk} \;;\; \Delta P_N = \sum_{j \in N} \Delta P_{mj} \,. \tag{10}$$

Now, the distribution of ΔP_C among CMs and of ΔP_N among NMs has many degrees of freedom, depending on the

[3] The compensation schemes portrayed in Figs 4b and 4c were proposed by Y. Zhang [16].

rescheduling conditions sought. For example, when the concern is to keep the overall system generation unchanged, the condition [4]

$$\Delta P_N = -\Delta P_C \tag{11}$$

yields, according to eq. (9) :

$$\Delta P_N = -\Delta P_C = -\Delta P_m = \Delta P. \tag{12}$$

In the case of contingency Nr 672 considered in Fig. 5, the computation of ΔP_m via expression (8) yields 91 MW, vs 85 MW provided by a pure (but much more tedious) time-domain procedure.[5] Hence, according to eq. (12), stabilizing this contingency implies decreasing the generation of the critical machine (Nr 2712) by 91 MW and increasing the generation of non-critical machines by the same amount (neglecting change of losses).

The above considerations are further elaborated below, in both cases of single and multi-machine critical clusters.

3.3 *Generation rescheduling w.r.t. a single contingency*

3.3.1 Principle

For a single unstable contingency, the stabilization procedure via the generation control of § 3.2 consists of computing the corresponding (negative) margin and from there ΔP_C and ΔP_N defined by (8), (12). The second step concerns the generation allocation of ΔP_C among CMs, whenever there are many, and of ΔP_N among NMs. Observe that the ΔP value computed via eq. (8) is only approximate; hence, its accurate assessment requires an iterative procedure.

Experience shows and engineering common sense suggests that the efficiency of this iterative procedure depends only marginally on the choice of NMs for reallocating generation of ΔP_N (though it may be of great importance with respect to other concerns such as maximum power transfer or economy, see Section 4). But it depends significantly on the way the ΔP_C generation is reallocated among CMs. A convenient way consists of reallocating ΔP_C according to the degree of criticalness of the critical machines. In turn, it seems reasonable to appraise this degree by the product M * g , and to write :

$$\frac{\Delta P_{ck}}{\Delta P_{cj}} = \frac{M_k g_k}{M_j g_j} \tag{13}$$

where M_k denotes the inertia coefficient of the k-th critical machine, ΔP_{ck} the corresponding generation decrease, and g_k its angular deviation with respect to the most advanced NM at time t_u .

A final observation relating to the iterative nature of the procedure : since, by construction, SIME proceeds mainly with negative, rather than positive margins, it is advisable to consider ΔP values somewhat (e.g. 10 %) smaller than those computed from eq. (8). This is clarified below.

[4] neglecting variation of losses.

[5] This 7 % discrepancy is because of neglecting the area A_8 between curves $P_e^{P'}$ and P_e^P ; indeed, the computation of this area provides 6 MW.

3.3.2 Resulting iterative procedure

The iterative procedure uses the following pattern :

(i) for a given clearing time and operating condition for which the CM's generation is P_1 , compute η_1 by SIME, then assess ΔP_1 by the compensation scheme of Fig. 5;

(ii) reallocate power and run a new power flow with $P_2 = P_1 - \Delta P_1$, and, further, run SIME to assess the corresponding η_2 ;

(iii) extrapolate (or interpolate, as appropriate) the pair (η_1, η_2) to find the new power limit P_3 , and compute η_3 ;

(iv) proceed as in step (iii), using the pair (η_2, η_3) ;

(v) repeat step similar to (ii), (iii) until reaching $\eta = 0$.

The procedure converges rapidly, as shown in Section 5.

3.4 *Generation rescheduling w.r.t. a set of contingencies*

To stabilize the whole set of dangerous contingencies *simultaneously*, the procedure of § 3.3. may be adapted as follows.

(i) For a given unstable contingency : compute the decrease in generation of the critical group of machines following the procedure of § 3.2, and

- if this group contains a single CM : impose this decrease on that CM
- if this group contains many CMs, distribute the amount of decrease in generation according to eq. (13);

(ii) proceed likewise with all unstable contingencies

(iii) for each CM, choose the generation decrease to be the maximum among those computed in above steps (i), (ii);

(iv) compute the total generation decrease obtained for all CMs, and compensate by an equal generation increase in NMs. The choice of NMs and the amount of power increase for each one of them may follow various rules depending on the objective sought; e.g., in the MAT method described in next section, the aim is to provide maximum allowable transfer between preassigned areas.

4 Applications to on-line DSA and control

4.1 *The MAT method [12]*

4.1.1 Problem statement

The "transient stability-constrained maximum allowable transfer" (for short MAT) method proposed in Ref. [12] addresses the following problem : "within time frames compatible with on-line operation, allocate power generation so as to maximize the power transfer between transient stability-limited power systems". This problem may be divided in the following sub-problems :

- set up the initial list of all contingencies likely to threaten the system transient stability
- specify the exporting and importing areas; determine, accordingly, the maximum power that can be transferred and the corresponding operating conditions
- screen the contingencies to select the potentially harmful ones, using the compensation technique of § 3.1

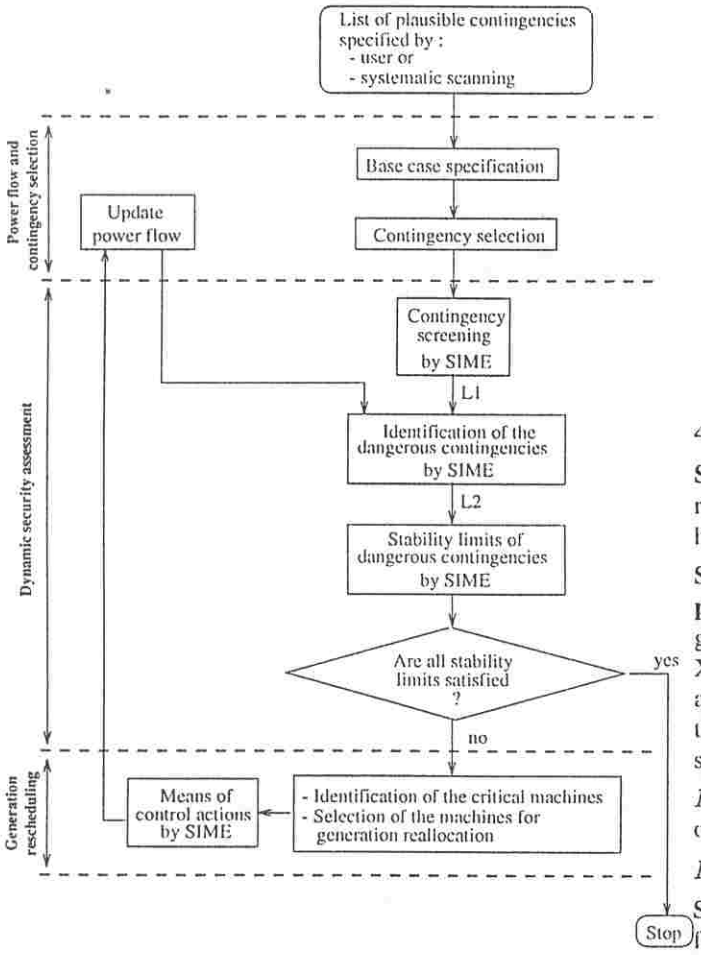

Figure 6. Structural organization of the MAT method

- under a preassigned clearing time, identify the actually "dangerous" ones, i.e., those which are unstable for this clearing time, compute their (negative) stability margin, and identify the corresponding critical machines
- assess control actions to stabilize all dangerous contingencies simultaneously, by decreasing generation on critical machines according to § 3.4.
- reallocate generation so as to maximize the power transferred between areas, consider rules of § 4.3.

Figure 6 describes the structural organization of the proposed method and the corresponding tasks, elaborated below.

4.1.2 Specification of maximum allowable transfer

The tie-lines on which large amounts of power have to be transferred are determined by specifying the exporting and importing areas. They are labelled as X and Y respectively in Fig. 7; the additional areas which may be involved (the"dummy areas") are labelled as "Z".

To determine the maximum allowable transfer on the tie-lines thus specified, a base-case scenario is considered where areas X and Y operate under highly stressed conditions, by increasing the generation in area X up to its maximum level, and decreasing the generation in area Y down to its minimum level.

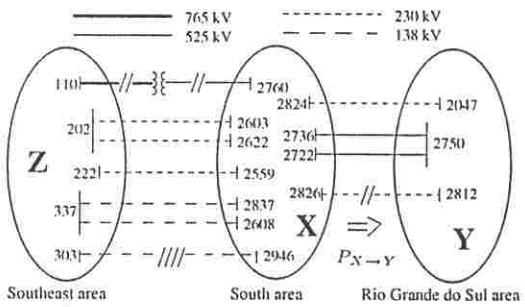

Figure 7. Interarea power flows in the Brazilian system

4.1.3 Selection rules for generation rescheduling

Selection rule 1 : generation limits. Obviously, the generation rescheduling (decrease for CMs, increase for NMs) should not hit the machines' lower and upper generation limits.[6].

Selection rule 2 : generation rescheduling for maximum power transfer. Given a set of CMs, and corresponding NMs, given an exporting and an importing area (labelled as areas X and Y respectively), and given the control actions on CMs advocated in § 3.4, the purpose is to ensure the largest possible tie-line power transfer $P_{X\rightarrow Y}$ by properly selecting NMs. This selection takes into account that :

$P_{X\rightarrow Y}$ is either increased or unchanged, when acting on NMs of area X or Z

$P_{X\rightarrow Y}$ is decreased, when acting on NMs of Y.

Selection rule 3. Generally, Selection rules # 1 and 2 leave some freedom, especially in the choice among NMs. For instance, the cost of generation may be taken into account.

4.2 *On-line transient stability monitoring*

Traditionally, security monitoring has been limited to steady-state security aspects. The generation limits derived in § 3.3 may be easily extended for security monitoring to include transient stability as well. The simulations of § 5.5 illustrate the resulting procedure.

5 A real-world example

5.1 *Simulation description*

Study scenario. The South-Southeast Brazilian power system is modelled with 56 machines, 1188 buses and 1962 lines, the voltage levels ranging from 138 to 765 kV. Figure 7 portrays schematically the interconnections of this system.

The purpose of the simulations is threefold :

- to compare the best compensation schemes for controlling clearing time and show their effectiveness as screening tools
- to illustrate the control of generation for dangerous contingencies, considered individually
- to illustrate the control of generation for dangerous contingencies, considered simultaneously.

[6]Note that in the extreme case of unfeasible solutions (i.e. when all machines are already operating at their limits), the method would be led to suggest extreme actions of generation and load shedding.

Table 1. Operational data of the power plants

1	2	3	4	5	6	7
Mach. #3	Init.gen. (MW)	Final gen. (MW)	Min.gen. (MW)	Max.gen. (MW)	Gen.cost (US$/MWh)	Area (area)
23	333	371	180	400	12.68	Z
24	237	325	180	400	12.68	Z
291	102	124	0	132	12.68	Z
404	109	127	0	140	12.68	Z
405	62	72	0	80	12.68	Z
406	84	97	0	108	12.68	Z
2573	248	246	0	248	24.39	X
2705	122	119	60	122	41.58	X
2706	250	213	160	250	37.30	X
2707	350	299	158	350	36.18	X
2712	1050	953	780	1050	24.39	X

The base case considered here corresponds to a peak load scenario forecasted for 1998[7], in which a large amount of power is being injected into Rio Grande do Sul area, operating with an important generation deficit.

In addition, in this latter case, the concern of § 5.4 is to transfer the maximum power to the Rio Grande do Sul area (Y) from the South area (X) which is connected to and supplied from the Southeast area (Z).

Power system modelling. Two types of models are considered, namely : (i) the standard simplified model (SM), where each machine is represented by constant mechanical power and constant electromotive force behind transient reactance; (ii) a detailed model (DM), where all the machines are represented with full model (IV-IEEE model) and with controls (AVRs in 46 machines, PSSs in 8 machines and prime movers/governors in 7 machines of thermal plants). Both SM and DM models use constant impedance load representation. The maximum simulation time for the time-domain program is of 2 seconds for SM and 5 seconds for DM.

Contingency type and location. The contingencies considered are three-phase short-circuits. They are successively applied at all 138 kV up to 525 kV buses of areas X and Y, and subsequently cleared by opening one line or transformer adjacent to the faulted bus. This yields a total of 712 contingencies.

Additional information. The time-domain simulations are performed with the ST600 program of Hydro-Québec [17]. The threshold clearing time for identifying dangerous contingencies is arbitrarily fixed to 167 ms (10 cycles); actually, this is much larger than that used in practice. All generation units are in operation. Table 1 reports on operational data of those power plants which concern the simulations performed.

5.2 *Contingency selection, assessment ranking*

The initial list of 712 contingencies are screened as indicated in Fig. 8 : the first filtering step using simplified model discards 644 (90 %), and retains 68 contingencies; the second step using detailed model eliminates 45 out of the 68 contingencies, and "sends" to the assessment phase 23 "potentially harmful" contingencies (i.e., having CCTs smaller than 200 ms), which thus compose the list L1.

[7] of 32,538 MW

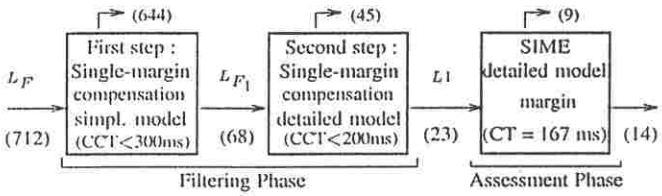

Figure 8. Automatic contingency selection

Finally, the potentially harmful contingencies are scrutinized in the "assessment phase", by computing their margins, obtained with a clearing time of 167 ms. It shows that among the 23 potentially harmful contingencies, 14 are actually dangerous.

Table 2 gathers information about the second filtering step and the assessment phase, for the 23 contingencies found to be potentially harmful. More precisely, columns 4 and 5 provide the CCT values (t_{c3}, t_{c4}) obtained with the compensation schemes of Figs 4c and 4d, using the margin of column 3; this margin is obtained for the clearing time indicated in column 2, automatically selected by SIME. Observe that apart from contingency Nr 672, the computation of each one of the other margins required a sole unstable time-domain integration, the mean duration of which is about 500 ms.

Inspection of columns 4 and 5 suggests that the approximate CCT of the selected 23 contingencies is below 200 ms, and are, therefore, potentially harmful; hence, they are sent to the full SIME for more accurate assessment. The result is given in column 6 which lists the margin values corresponding to a clearing time of 167 ms. Obviously, the first 14 contingencies of the list are, indeed, dangerous, since they have a negative margin.

Another way of filtering contingencies by assessing their approximate CCT is to use the pair of margins of columns 3 and 6. The CCTs of the resulting two-margin filter are reported in column 7. It is interesting to compare them with those obtained with the single-margin ones of columns 4 and 5.

For the sake of further comparisons, column 8 provides the CCT assessed by the full SIME, while column 9 the CCT assessed by the ST-600 time-domain program, used as the reference.

5.3 *Generation rescheduling w.r.t. each dangerous contingency*

Table 3 collects the main results of simulations, which consider separately each one of the 14 dangerous contingencies of Table 2.

Iteration # 1 : Column 2 lists the normalized margins η_1 in $(\text{rad/s})^2$, as computed by SIME for a clearing time of 167 ms. Column 3 provides the corresponding total generation change provided by the compensation scheme of § 3.2, ΔP_1 , by which the critical cluster should be decreased. If this cluster comprises many CMs, the power reallocation is determined according to (13). Column 4 collects information about the resulting generation reallocation among CMs; thus, for a given contingency, one reads in a row : the name of the CM followed between brackets by the gap between this CM and the most advanced NM, and

Table 2. Results of second filtering step and of SIME

1	2	3	4	5	6	7	8	9
Cont.	Clear. time (ms)	Margin corresp. to CT of Col.2	t_{c3} (ms)	t_{c4} (ms)	Margin corresp. to CT of 167 ms	CCT filt. (ms)	CCT SIME (ms)	CCT Ref. (ms)
687	210	-54.7	160	165	-23.9	134	117	117
656	210	-42.7	122	132	-17.1	138	132	132
686	225	-46.3	177	181	-12.4	146	135	138
672	250,227	-57.8	123	136	-14.7	146	140	143
630	210	-37.4	151	157	-15.6	151	147	147
680	250	-74.0	1375	158	-9.7	154	149	152
708	250	-73.4	136	156	-9.4	155	151	152
598	250	-73.9	133	154	-9.4	155	151	152
629	210	-37.8	152	158	-16.5	157	154	152
463	250	-73.9	131	152	-8.0	157	155	152
692	210	-36.2	155	160	-4.9	160	155	157
707	250	-73.4	139	159	-6.7	159	160	157
690	225	-37.7	161	168	-2.4	163	160	162
437	215	-100.1	155	163	-1.1	167	166	162
434	215	-96.3	160	167	45.1	152	170	168
628	225	-33.8	175	180	24.1	191	171	173
689	225	-33.2	176	180	24.0	195	173	173
362	225	-32.8	177	181	27.4	193	176	178
522	215	-92.7	167	173	70.2	188	176	173
516	215	-83.6	176	180	98.0	193	182	183
669	275	-24.1	165	176	22.1	219	204	216
626	270	-44.7	192	201	37.0	214	212	216
668	275	-19.5	196	203	23.2	226	218	228

the generation decrease resulting from the proportionality rule (13).

Iteration # 1 requires one stability margin computation per contingency, preceded by one load flow (LF), common to all contingencies.

Iteration # 2 : At the end of Iteration # 1, a LF is run for each contingency, in order to take into account the power increase on CM(s) and the same amount of power decrease on NMs. (E.g., for contingency Nr 672, a decrease of 82 MW is imposed on machine Nr 2712). This LF is followed by a SIME's computation of the new margin value (-0.5 for the case 672). Further, extra-(inter-)polating margins η_1 and η_2 provides a new ΔP value by which the generation of CM(s) should be modified (-3 MW for the case 672). Finally, running a new LF with this new generation power provides the actual generation power limit for stabilizing the contingency, i.e. for increasing its CCT to 167 ms.

Thus, Iteration # 2 requires 2 LFs and 1 stability margin computation per contingency.

Observe that this iteration is also the final one; indeed, columns 4 and 5 indicate that attempting to improve the stabilization of contingencies with negative values for η_2 , provides negligible corrections, ΔP_2 .

Remark. The main concern of the above procedure is to show that the compensation scheme of § 3.2 works, indeed, satisfactorily (i.e. provides proper ΔP_1 values). From a practical point of view, however, the concern is how to stabilize all contingencies simultaneously rather than individually. This latter question is addressed below.

Table 3. Case-by-case rescheduling procedure. Generation decrease distributed among CMs

Iteration # 1			
1	2	3	4
Cont. #	η_1 (rad/s)^2	ΔP_1 (MW)	CM (gap (°); ΔP (MW))
687	-23.9	-70	2707(53;-42);
			2706(41;-28);
656	-17.1	-71	2707(112;-31);
			2706(101;-24);
			2705(90;-11);
			2704(56;-5);
686	-12.4	-38	2707(53;-20);
			2706(48;-18);
672	-14.7	-82	2712 (89;-82)
630	-15.6	-45	2707(31;-45)
680	- 9.7	-52	2712(94;-52)
708	- 9.4	-50	2712(96;-50)
598	-9.4	-50	2712(95;-50)
629	-16.5	-31	2706(21;-31)
463	-8.0	-43	2712(94;-43)
692	-4.9	-19	2706(43;-7);
			2705(40,-4);
			2707(38,-8)
707	-6.7	-35	2712(95;-35)
690	-2.4	-10	2705(46;-3);
			2706(41;-4);
			2707(27;-3)
437	-1.1	-2	2573(103;-2);
Iteration # 2			**Iteration # 3**
1	2	3	4	5
Cont. #	η_2 (rad/s)^2	ΔP_2 (MW)	η_3 (rad/s)^2	ΔP_3 (MW)
687	-2.2	-7	0.3	1
656	2.3	8		
686	-1.3	-4	0.09	~ 0
672	-0.5	-3	0.07	~ 0
630	2.2	6		
680	-0.2	-1	-0.01	~ 0
708	-0.7	-4	-0.04	~ 0
598	-0.6	-3	-0.04	~ 0
629	1.1	2		
463	-0.09	-1		
692	0.9	1		
707	-0.09	-1		
690	0.5	2		
437	1.7	1		

5.4 *Simulation results of the MAT method*

5.4.1 Iterative search of stability conditions

Iteration # 1

This iteration is identical with that of Table 3; the only difference is that, here, the purpose is to stabilize all dangerous contingencies *simultaneously*. To this end, the amount of power decrease on each CM is chosen to be the largest among those listed in Column 4 for all contingencies. This value is indicated in bold in Table 4.[8]

The resulting total generation decrease on all 6 CMs is the sum of the 6 values listed in bold, and amounts to 176 MW.

[8]Observe that there are 6 CMs for the 14 dangerous contingencies.

Table 4. Simultaneous rescheduling procedure

Iteration # 1				Iter. # 2	
1	2	3	4	5	6
Cont.	η_1 (rad/s)^2	ΔP_1 (MW)	CM (gap; ΔP)	η_2 (rad/s)^2	ΔP_2 (MW)
687	-23.9	-70	2707(53;-42); 2706(41;-28);	1.4	4
656	-17.1	-71	2707(112;-31); 2706(101;-24); **2705(90;-11); 2704(56;-5);**	3.1	14
686	-12.4	-38	2707(53;-20); 2706(48;-18);	7.7	29
672	-14.7	-82	**2712 (89;-82)**	-0.7	-4
630	-15.6	-45	**2707(31;-45)**	8.9	16
680	- 9.7	-52	2712(94;-52)	4.3	25
708	- 9.4	-50	2712(96;-50)	4.0	25
598	-9.4	-50	2712(95;-50)	4.1	25
629	-16.5	-31	**2706(21;-31)**	13.9	14
463	-8.0	-43	2712(94;-43)	5.8	34
692	-4.9	-19	2706(43;-7); 2705(40,-4); 2707(38,-9)	15.4	44
707	-6.7	-35	2712(95;-35)	7.2	42
690	-2.4	-10	2705(46;-3); 2706(41;-4); 2707(27;-3)	14.8	75
437	-1.1	-2	**2573(103;-2);**	1.7	1

To reallocate these 176 MW according to selection rules # 1 and 2 of § 3.4, consider the location of the various NMs (see Table 1); observing that area Z contains NMs, it is decided to act on these latter in order to avoid decreasing $P_{X \to Y}$.

Further, here, the choice among NMs of area Z takes into account generation cost (selection rule #3). The "cheapest" machines of area Z (with same generation cost) are listed in rows 1 to 6 of Table 1. The method therefore reallocates the 176 MW proportionally to their capacity.

Iteration # 1 requires one stability margin computation per contingency.

Iteration # 2

With the above generation rescheduling, a power flow program is run to determine the new operating state. Then, SIME is run to assess existence and severity of dangerous contingencies; thus, with a clearing time of 167 ms :

- if the contingency is found to be stable, the simulation is stopped after reaching δ_r (see § 2.4);[9]
- otherwise, the margin is computed; further, margins η_1 and η_2 are extra-(inter-)polated to determine the new value of generation reallocation of the corresponding critical group of machines, ΔP_2 , corresponding to zero margin (column 6).

Considering that the CMs and the proportionality rule used at Iteration # 1 still hold valid for borderline stable cases, yields

[9]Actually, the first simulation of a stable case is extended to the entire integration period, to avoid missing a multiswing instability. This "costs" a whole time-domain simulation for each selected contingency, i.e., comparatively, quite a considerable CPU time.

Table 5. Tie-line flows at successive iteration steps

1	2				3	4
Iter.	Tie-line flows (MW)				Total flow	Losses
	2736-2750	2722-2750	2824-2047	2826-2812	(MW)	(MW)
1	945	790	189	230	2154	1778
2	958	803	168	225	2153	1765
3	958	802	169	224	2153	1763

the following values of generation reallocation (see column 6) : CM(2573) = +1 ; CM(2704) = +1 ; CM(2705) = +2 ; CM(2706) = +2 ; CM(2707) = +2; CM(2712) = -4 . These values are marginally positive (and the corresponding cases marginally overstabilized) except for contingency Nr 672 (CM(2712)) which is marginally understabilized. One thus may decide to run a new power flow with the above corrections without any further stability run. Indeed, this run would provide marginal changes only; for instance, for contingency Nr 672, this provides $\eta_3 = 0.12\,(\text{rad/s})^2$, $\Delta P_3 = 0.5\,\text{MW}$.

Thus, Iteration # 2 requires one stability margin computation per contingency and two power flows.

Final check

With the above generation rescheduling, SIME is run to check that none of the 712 contingencies is anymore or has become dangerous.

5.4.2 Iterative search of maximum tie-line flows

Table 5 summarizes the changes in the tie-line flows during the iterative procedure of § 4.1. According to Column 3 of this table, the total tie-line flow from area X to area Y is finally decreased by only 1 MW (0.05 %) with respect to its initial value, thanks to the existence of NMs in area Z. Thus, rescheduling the generation in the power system has significantly improved the system transient stability, without affecting (except marginally) the maximum tie-line transfer.

5.4.3 Generation cost

Incidentally, observe that the generation decrease of the CMs of area X (which are more expensive) and the generation increase of NMs of area Z (which are less expensive) result in a decrease in the overall generation cost of 3,490 US$ per hour.

5.5 *On-line transient stability monitoring*

The MAT method illustrated above ensures maximum power transfer within transient stability limits. Another issue of great concern is the maximum power that the system generators may deliver within transient stability limits. The computation of these generation limits may be achieved by SIME in various ways, depending upon the particular objective sought.

The computation reported below is chosen for the sake of convenience, in order to take advantage of results already obtained in the context of the MAT method. It consists of: (i) considering the dangerous contingencies identified in § 5.2; (ii) appraising, for each one of them, the amount of generation decrease necessary to stabilize it; in case there are more than one CMs, the exercise is repeated separately for each one of them. The actual excess of generation carried by each critical generator is the maximum among the values computed for the various

Table 6. Case-by-case rescheduling procedure. Generation decrease reported on a sole CM.

1	2	3	4	5	6
Cont. and CMs	Compens. m/nes	Gen. power (MW)	Margin η	ΔP (MW)	Final power produced by CMs 2707 + 2706
687	2707	350	-23.9	-70	
		280	-0.7	-2	
2707		278	Stable		278 + 250 = 528
2706	2706	250	-23.9	-70	
		180	-8.56	-39	
		141	Stable		350 + 141 = 491
656	2707	350	-17.1	-71	
		279	Stable		279 + 250 = 529
2707, 2706,	2706	250	-17.1	-71	
2705, 2704		179	-2.8	-14	
		165	Stable		350 + 165 = 515
686	2707	350	-12.4	-38	
		312	-.01	-0.03 $\simeq$ -1	
2707		311	Stable		311 + 250 = 561
2706	2706	250	-12.4	-38	
		212	-3.2	-13	
		199	Stable		350 + 199 = 549
692	2706	250	-4.9	-19	
		231	Stable		350 + 231 = 581
2706, 2705,	2707	350	-4.9	-19	
2707		331	Stable		331 + 250 = 581
690	2706	250	-2.4	-10	
		240	Stable		350 + 240 = 590
2705, 2706,	2707	350	-2.4	-10	
2707		340	Stable		340 + 250 = 590

Table 7. Accuracy assessment of tie-line flows

	Tie-line flows (MW)				Tot. interface
Method	2736-2750	2722-2750	2824-2047	2826-2812	flow (MW)
MAT	958	802	169	224	2153
ST600	957	801	171	224	2153

contingencies. Table 6 collects the results obtained with the 5 dangerous contingencies which have more than one critical machine; the stabilization is obtained by acting only on the generation power of machines 2706 and 2707. Column 6 compares the maximum active power that the CMs can produce after stabilization. Observe that stabilizing the most advanced (and hence most unstable) machine does not necessarily yield the maximum power.

As an illustration, Fig. 9 shows the region of stable operating conditions of the system, in terms of the active power output of critical machines 2706 and 2707, for contingency 687. This region is bounded by dotted and solid lines. These lines represent the limit value of the active power of one machine, considering that the active power of the other machine remains constant. For example, the solid line is the limit value of machine 2706 active power (141 MW) when machine 2707 produces 350 MW. The dotted line is the limit value of machine 2707 active power (278 MW) when machine 2706 generates 250 MW. The resulting overall stability region is the shaded area of Fig. 9. These limits are also the limits of the critical generators' active power for the set of contingencies with more than one critical machine (687, 656, 686, 692, 690).

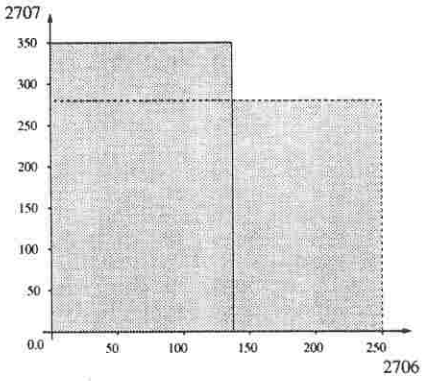

Figure 9. Region of stable operating conditions of the system for contingency 687 in terms of the active power of machines 2707 and 2706

5.6 *Performances*

5.6.1 Accuracy performances of MAT

The accuracy of the filtering steps is checked using the time-domain program (with simplified and detailed power system models, as appropriate). It is found that all discarded contingencies are, indeed, harmless, i.e. that their actual CCTs are larger than the adopted threshold values.

Similarly, as a validation of the overall MAT procedure, the CCTs of all 712 cases are again simulated at the end of the procedure by a pure time-domain program : they are found to be consistently larger than the CCTs "before" MAT.

Further, the ST600 program, used as the reference, checks SIME's accuracy in the different steps of the MAT procedure in terms of CCTs and power limits. ST600 verifies that SIME is, indeed, very accurate. Table 7 compares the power flows in all tie-lines as provided by MAT and by ST600, and shows that they are in total agreement.

5.6.2 CPU requirements

A precise assessment of CPU times is not easy. Instead, one may proceed by comparisons. Such a handy measure for comparisons is the number of equivalent *seconds of time-domain integration* (sTDI for short) of the transient stability program.

A very rough indication of computing requirements is given below, considering separately various steps of the MAT and the on-line transient stability monitoring procedures.

Filtering phase

- First filtering step: this step requires slightly more than 712 unstable time-domain runs for computing the 712 margins and resulting t_{c3}, t_{c4} ; each one of the unstable time-domain runs amounts to about 500 ms of time-domain integration with simplified power system model (see comments of § 5.2). this yields about 370 seconds of time-domain integration with simplified model.
- Second filtering step: according to § 5.2, this step requires about $0.5 \times 69 \simeq 35$ sTDI with detailed model.

Assessment step

Computation of the stability margins of the potentially harmful contingencies by SIME $\simeq 23 \times 0.5 = 12$ sTDI.

Iterative MAT procedure: $2 \times 14 \times 0.5 = \mathbf{14\,sTDI}$.

Additional computations: in addition to the above computations, one should take into account those required for running power flows, for the compensation schemes, and for computing the OMIB parameters. All these computations would amount to about 1 or 2 sTDI.

Observe that the computations of the most time-consuming tasks may easily be distributed and carried out in parallel; hence the MAT CPU times may be fully compatible with requirements for real-time preventive monitoring and control.

6 Acknowledgements

The first author gratefully acknowledges the financial support of the Consejo Nacional de Ciencia y Tecnologia, México for his PhD studies.

7 Conclusion

This paper has explored various types of on-line techniques for transient stability-constrained power limits, relating to the emerging ATC arena. The techniques rely on the SIME method and consist of assessing the maximum allowable generation of the critical machines and, whenever necessary, of decreasing their generation while rescheduling generation of non-critical machines.

The rescheduling may comply with various requirements, such as maximum transfer between areas or generation cost. It may be handled by an optimal power flow program.

The final stage of this research aims at devising a fully automatic approach, by coupling SIME, used to assess the critical machines' generation, with an OPF, used to reschedule the generation of non-critical machines. This is now in good progress.

8 References

[1] Gross G. (Editor), *Proceedings of the Workshop on Available Transfer Capability*, University of Illinois at Urbana-Champaign, June 26-28, 1997.

[2] Brandwajn V., A.B.R. Kumar, A. Ipakchi, A. Bose and S. Kuo (1997), "Severity indices for contingency screening in dynamic security assessment", *IEEE Transactions on Power Systems*, Vol.12, No.3, pp. 1136-1142.

[3] Ejebe G.C. , C. Jing, J.G. Waight, G. Pieper and F. Jamshidian (1996), "Security monitor for on-line dynamic security assessment", *Proc. of Power System Control and Management*, April, pp. 58-64.

[4] Fouad A.A. and T. Jianzhong (1993), "Stability constrained optimal rescheduling of generation", *IEEE Transactions on Power Systems*, Vol.8, No.1, pp. 105-112.

[5] Hwang C. , V. Vittal and A.A. Fouad (1989), "Determination of interface flow stability limits by sensitivity analysis of transient energy margin", *IFAC Symposium on Power System and Power Power Plant Control*, Seoul (Korea), Aug., pp. 189-194.

[6] Kuo D.H. and A. Bose (1995), "A generation rescheduling method to increase the dynamic security of power systems", *IEEE Transactions on Power Systems*, Vol.10, No.1, pp. 68-76.

[7] Ejebe G.C. *et al.*, "On-line dynamic security assessment in an EMS". In *IEEE Computer Applications in Power*, Vol. 11, No. 1, January 1998.

[8] Xue Y., Th. Van Cutsem and M. Ribbens-Pavella, "A real-time analytic sensitivity method for transient security assessment and preventive control", *IEE Proc. C*, Vol. 135, No 2, pp. 96-107.

[9] Xue Y. (1988), "Transient stability limits of interface flows". *IFAC Symposium on Power System Modelling and Control*, Brussels (Belgium), Sept., pp. 3.2.1.-3.2.6.

[10] Xue Y., " Practicaly negative effects on emergency controls", *Proc. of IFAC/CIGRE Symp. on Control of Power Systems and Power Plants, Beijing, China*, pp. 649-654.

[11] Ernst D., A.L. Bettiol, D. Ruiz, L. Wehenkel, and M. Pavella, "Compensation schemes for transient stability assessment and control". *LESCOPE '98*, Halifax, June 7-9, 1998, pp. 225-230.

[12] Bettiol A.L., L. Wehenkel, and M. Pavella, " Transient stability-constrained maximum allowable transfer". Paper Nr 985SM334, *1998 PES/IEEE Summer Meeting*, San Diego.

[13] Pavella M., "Generalized one-machine equivalents in transient stability studies',' *PES Letters*, in *IEEE Power Engineering Review*, Vol.18, No. 1, January 1998, pp. 50-52.

[14] Zhang Y., L. Wehenkel, P. Rousseaux and M. Pavella, "SIME : a hybrid approach to fast transient stability assessment and contingency selection," *Journal of EPES*, Vol.19, No.3, 1997, pp. 195-208.

[15] Zhang Y., L. Wehenkel and M. Pavella, "SIME : A comprehensive approach to fast transient stability assessment," *IEE of Japan*, Vol. 118-B, No.2, January 1998, pp. 127-132.

[16] Zhang Y., "Approximating critical clearing times using compensation schemes," Private communication, January 1997.

[17] Valette A., F. Lafrance, S. Lefebvre and L. Radakovitz, " ST600 programme de stabilité : manuel d'utilisation version 701," *Hydro-Québec, Vice-présidence technologie et IREQ*, 1987.

9 Biographies

Daniel Ruiz Vega received the Electrical Engineering degree from the Universidad Autonoma Metropolitana (Mexico) in 1991 and the M.Sc. degree from the Instituto Politecnico Nacional (Mexico) in 1996. He is presently a Ph.D student at the University of Liege (Belgium).

Arlan Luiz Bettiol received the electrical engineering degree in 1988 and the M.Sc. degree in 1992 both from the University of Santa Catarina (Brazil). He is presently a Ph.D student at the University of Liège, Belgium. His research concerns dynamic security assessment.

Damien Ernst was born in Verviers, Belgium, in 1975. He is currently a student at the electromechanical engineering department of the University of Liège, nearing completion of his undergraduate studies. He has been working for about two years on SIME.

Louis Wehenkel received the Electrical (Electronics) engineering degree in 1986 and the Ph.D degree in 1990 both from the University of Liège, Belgium, where he is presently a research associate of the F.N.R.S. His research concerns power system security analysis and control.

Mania Pavella received the Electrical (Electronics) engineering degree and the Ph.D degree both from the University of Liège, where she is presently a Professor. Her research interests lie in the field of electric power system analysis and control.